Available online at www.sciencedirect.com
ScienceDirect
Ceramics International 35 (2009) 1775–1781
CERAMICS INTERNATIONAL
www.elsevier.com/locate/ceramint

Synthesis, microstructure and electrical conductivity of carbon nanotube–alumina nanocomposites

L. Kumari [a], T. Zhang [a], G.H. Du [a], W.Z. Li [a,*], Q.W. Wang [b], A. Datye [c], K.H. Wu [c]

[a] *Department of Physics, Florida International University, Miami, FL 33199, United States*
[b] *Agiltron Inc., 15 Cabot Road, Woburn, MA 01801, United States*
[c] *Mechanical and Materials Engineering, Florida International University, Miami, FL 33174, United States*

Received 1 September 2008; received in revised form 12 September 2008; accepted 1 October 2008
Available online 21 October 2008

Abstract

Carbon nanotube–alumina (CNT–Al_2O_3) nanocomposites have been synthesized by direct growth of carbon nanotubes on alumina by chemical vapor deposition (CVD) and the as-grown nanocomposites were densified by spark plasma sintering (SPS). Surface morphology analysis shows that the CNTs and CNT bundles are very well distributed between the matrix grains creating a web of CNTs as a consequence of their in situ synthesis. Even after the SPS treatment, the CNTs in the composite material are still intact. Experimental result shows that the electrical conductivity of the composites increases with the CNT content and falls in the range of the conductivity of semiconductors. The nanocomposite with highest CNT content has electrical conductivity of 3336 S/m at near room temperature, which is about 13 orders of magnitude increase over that of pure alumina.

Keywords: A. Sintering; B. Nanocomposites; C. Electrical conductivity; Chemical vapor deposition; Carbon nanotubes

1. Introduction

Carbon nanotubes (CNTs) have been investigated extensively for the past decade to explore their unique physical properties and many potential applications. One of the most promising uses of CNTs is in the development of nanocomposites, where the CNTs are used as novel fillers and binders to improve their mechanical, electrical and thermal properties [1–3]. CNTs have great potential applications due to their very large aspect ratio (1000–10,000) [4], low density, high rigidity (Young's modulus of the order of 1 TPa) [5,6], and high tensile strength (up to 60 GPa) [7]. In addition, the excellent electrical conductivity (10^6 S/m at 300 K for single-walled CNT (SWCNT) and $>10^5$ S/m for multi-walled CNT (MWCNT)) [8,9] and thermal conductivity (6600 W/mK for an individual SWCNT and >3000 W/mK for an individual MWCNT) [10,3] make them suitable candidates in preparing nancomposities with new functional properties. Ceramics can sustain high temperature and have high hardness, but the most noted shortcoming is its inherent brittleness and highly insulating behavior, which has limited its extensive applications [11]. Thus CNTs are considered to be a promising component of a new class of CNT–ceramic composites, which may offer high mechanical, electrical and thermal performances unattainable from current composite materials.

CNT-reinforced ceramic nanocomposite has become an intriguing field of intense research. Most of the attempts have been made to improve the mechanical properties of composites through incorporating CNTs [12]. The electrical conductivity of CNT–polymer materials due to the percolation of CNT has been widely investigated [2,13–15], but only a few authors have reported the electrical conductivity of CNT–ceramic composites. Flahaut et al. [16] synthesized CNT–Fe–Al_2O_3, CNT–Fe/Co–$MgAl_2O_4$, and CNT–Co–MgO composites and measured their electrical conductivity which was in the range of 200–400 S/m owing to the percolation of the CNTs in the matrix material. Zhan et al. [17] obtained an electrical conductivity of 3345 S/m on the 15 vol% SWCNT–alumina nanocomposites, an increase of 13 orders of magnitude over that of pure alumina. Previous reports by Rul et al. [18] and

* Corresponding author. Tel.: +1 305 348 7257; fax: +1 305 348 6700.
E-mail address: Wenzhi.Li@fiu.edu (W.Z. Li).

0272-8842/$34.00
doi:10.1016/j.ceramint.2008.10.005

Ahmad et al. [19] independently investigated the electrical conductivity enhanced by CNTs in ceramic matrix nanocomposites and found a low percolation threshold of CNTs of 0.64 vol% for double-walled CNTs and 0.79 vol% for MWCNTs, respectively. These results have confirmed that CNTs provide efficient electrical discharge to insulating ceramic matrix [16–19] similar to what they do in an insulating polymer matrix. Hence, further investigation on the electrical conductivity enhancement provided by CNTs in ceramic-based nanocomposites is important.

The two key issues which are generally deemed as challenges to the introduction of CNTs into ceramic matrix composites are to (1) obtain homogeneous dispersion of CNTs in ceramics and (2) achieve a tight interface bonding between the CNTs and the surrounding matrix. These two issues are also critical for CNT–polymer composites, but are more crucial for ceramic matrix composites because of the entire incompatibility between the electrovalent bond of inorganic ceramic materials and the covalent bond of sp^2-bonded CNTs. Hence, preparation of well-dispersed CNT–ceramic powders and fabrication of isotropic CNT–ceramic composites in which CNTs are evenly distributed in bulk ceramics are main challenges to the fabrication process of CNT–ceramic composites. In the present study, we discuss the synthesis technique of CNT–Al_2O_3 nanocomposites. Here, the CNTs have been synthesized in situ on the Al_2O_3 ceramic grains and thus are very well distributed between the matrix grains. This technique also avoids any purification or dispersion treatments which could have altered the characteristics of the CNTs. Their microstructures and electrical properties have been investigated. The CNT addition induced enhancement in the electrical properties of the CNT–alumina nanocomposites has been discussed.

2. Experimental details

CNT–Al_2O_3 nanocomposites were synthesized by a chemical vapor deposition (CVD) method. The CNTs were directly grown on Al_2O_3 nanoparticles by using $Co(NO_3)_2{\cdot}6H_2O$ as catalyst precursor [20]. To upload the catalyst precursor on the Al_2O_3 nanoparticles, $Co(NO_3)_2{\cdot}6H_2O$ (98+%, Sigma–Aldrich) and Al_2O_3 powder (CR30 Al_2O_3 powder, Baikowski Inc., purity 99.99%) were mixed in ethanol, followed by sonication for 15 min. Then, the mixture was dried at 130 °C for overnight followed by grinding into a fine powder. The $Co(NO_3)_2{\cdot}6H_2O$ catalyst precursor was reduced by H_2 gas to metal Co particles which were distributed on the Al_2O_3 matrix particles and would act as catalysts for the growth of the CNTs. Four samples with weight ratio of Co/Al_2O_3 of 1.0, 2.0, 3.0 and 4.0 wt.% were prepared for the synthesis of CNT–Al_2O_3 composites.

For CNT synthesis, the Co/Al_2O_3 powder was placed directly in the fused quartz reaction tube. In the reaction tube, a fused quartz stirrer was used to stir the Co/Al_2O_3 powder to achieve a uniform exposure to the reaction gases and to obtain highly dispersed CNTs in the composite material. Acetylene (C_2H_2), hydrogen (H_2) and argon (Ar) with flow ratio of 1:4:6 were introduced into the reaction chamber through distilled water bubbler for CNT growth. The synthesis of CNTs was carried out at 750 °C for 15 min. After the synthesis, the CNT–Al_2O_3 composite material was placed in a 15-mm diameter graphite die and sintered under vacuum in a spark plasma sintering (SPS) unit (DR. SINTER spark plasma sintering system, SPS Syntex Inc.). The following conditions were applied in the SPS process: pressure 100 MPa, peak temperatures 1150 or 1450 °C, heating rate 100 °C/min, hold time at peak temperature 10 min, pulse duration 12 ms, and pulse interval 2 ms. For comparison, pure Al_2O_3 was also sintered at the same SPS conditions.

The final densities of the sintered nanocomposite samples were measured by the Archimedes method with deionized water as the immersion medium [21]. Microstructure analyses were performed using field emission scanning electron microscopy (FESEM, JEOL, JSM-6330F) and high-resolution transmission electron microscopy (HRTEM, JEOL 2010F). The electrical conductivity was measured using a four-point-probe technique carried out on a LCR Meter (Hewlett Packard/Model: 4263A) with resistance measurement accuracy of 0.001 mΩ. A cryogenics pump (CRYODYNE/Model: 22 refrigerators) and two cryogenics compressors (CT-CRYOGENICS/Model: 8200 compressor) were used to maintain the measurement temperature from 20 to 280 K controlled by a temperature controller (LAKESHORE/Model: 330 auto tuning) with a temperature measurement accuracy of 0.01 K.

3. Results and discussion

3.1. Microstructure analysis

Fig. 1 shows FESEM images of the CNT–Al_2O_3 nanocomposites after their growth in the reaction chamber. The growth conditions were the same for all the samples except for their Co catalyst contents. The four images (a), (b), (c), and (d) shown in Fig. 1 are corresponding to the nanocomposite samples with Co/Al_2O_3 ratios of 1.0, 2.0, 3.0, and 4.0 wt.%, respectively. From the FESEM images it is evident that the CNT content increases with the increase of the Co catalyst content. The well-distributed CNTs and their bundles are observed in the alumina matrix. As the Co content ratio reaches to 3.0 and 4.0 wt.% (Fig. 1c and d), high quantity of CNTs are presented. Due to the existence of large quantity of CNTs, some alumina particles are wrapped around by these CNTs. The yield of the CNTs grown on the 1.0, 2.0, 3.0, and 4.0 wt.% Co/Al_2O_3 samples are 7.39, 8.25, 18.82, and 19.10 wt.%, respectively. The diameter of CNTs is about 10–40 nm while their length is around 1–7 μm.

Fig. 2 shows the TEM and HRTEM images of CNTs grown in the 1.0 wt.% Co/Al_2O_3 matrix. TEM image (Fig. 2a) shows both the CNTs and the Al_2O_3 nanoparticles, and it clearly depicts that the CNTs are clean and curly and the Al_2O_3 nanoparticles still keep their original size and do not grow bigger during the CNT growth. Some CNTs have closed tips (not shown) in which Co catalysts are usually capped inside. This observation implies that the CNTs grown in the alumina

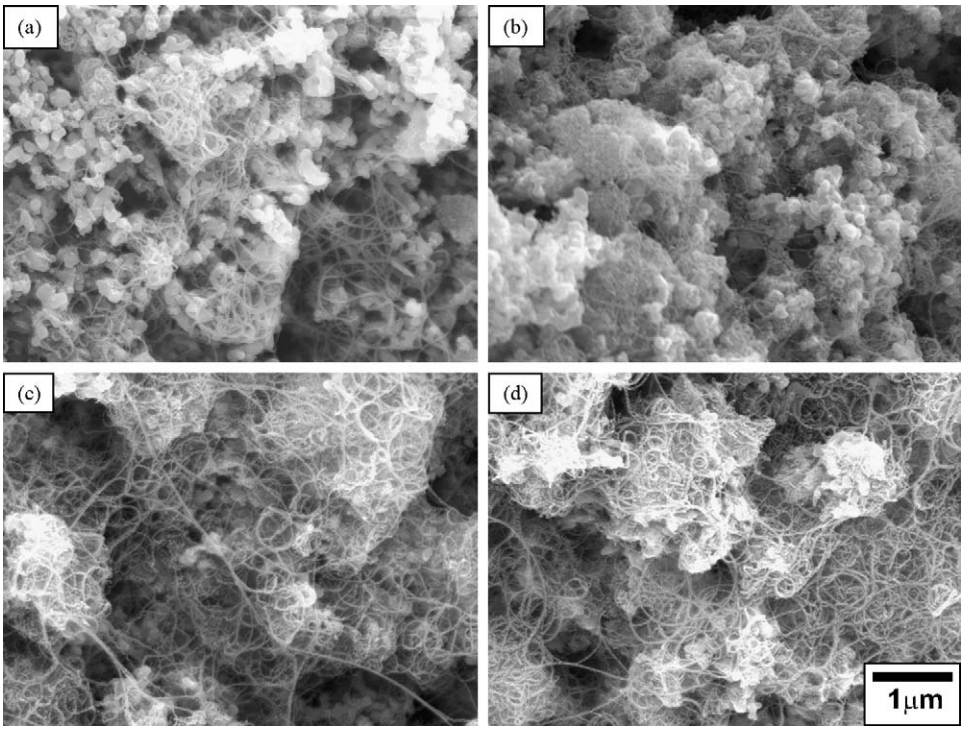

Fig. 1. FESEM images of CNT–Al_2O_3 nanocomposites with different CNT contents (a) 7.39 wt.%, (b) 8.25 wt.%, (c) 18.82 wt.%, and (d) 19.10 wt.%.

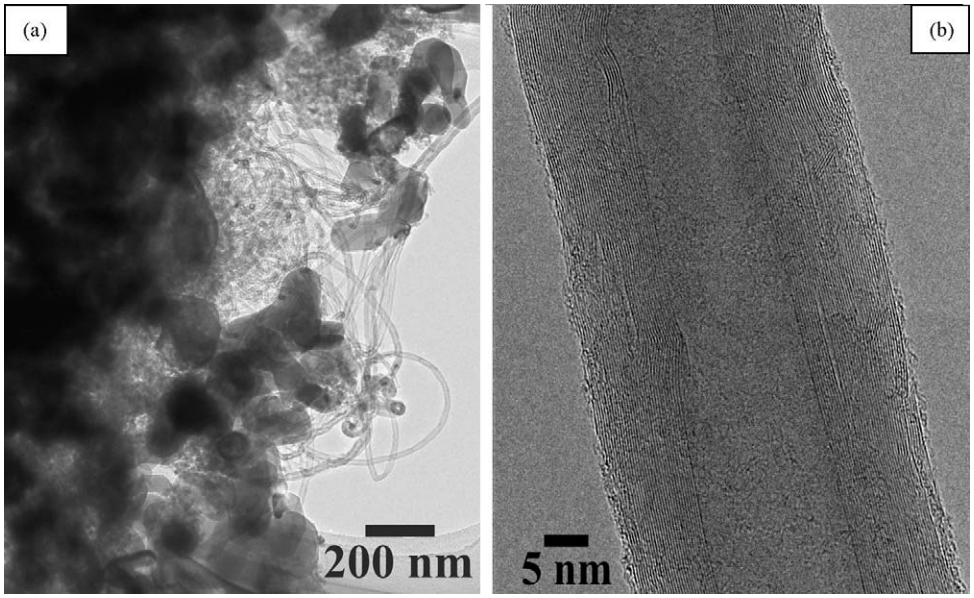

Fig. 2. TEM (a) and the corresponding HRTEM (b) images showing the morphology and size of CNTs in the 7.39 wt.% CNT–Al_2O_3 nanocomposite synthesized with 1.0 wt.% Co/Al_2O_3.

matrix are by tip growth mode [22]. HRTEM image of a single CNT in the nanocomposite sample is shown in Fig. 2b. HRTEM result shows that the CNTs in the nanocomposite are MWCNTs and usually have 10–40 walls.

Fig. 3a–d shows the fracture surfaces of the 7.39 and 19.1 wt.% CNT–Al_2O_3 nanocomposites sintered at 1150 and 1450 °C, respectively. The images showed that the CNTs survived from the quick high temperature SPS. Comparing the FESEM images of nanocomposites before (Fig. 1) and after (Fig. 3) SPS, no significant change in the morphology, quantity and distribution of CNTs is observed in the sintered nanocomposites. It clearly shows that the CNTs are clean and the Al_2O_3 nanoparticles still retain their original size and do not grow bigger during SPS treatment. From the images in Fig. 3, one can find that the composites sintered at low temperature of 1150 °C (Fig. 3a and c) have high porosity while

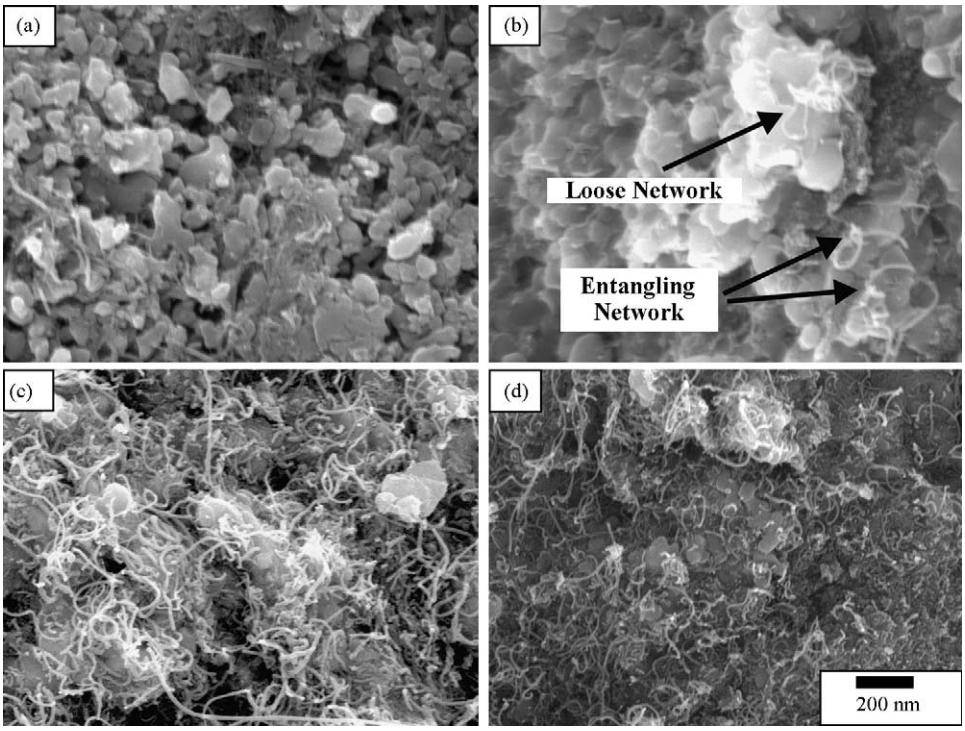

Fig. 3. Fracture surfaces of the CNT–Al_2O_3 nanocomposites sintered at different temperatures. The 7.39 wt.% CNT–Al_2O_3 sintered at (a) 1150 °C and (b) 1450 °C; the 19.1 wt.% CNT–Al_2O_3 nanocomposites sintered at (c) 1150 °C and (d) 1450 °C (scale bar 200 nm).

Table 1
Electrical conductivities of CNT–Al_2O_3 nanoncomposites and other ceramic-based CNT composites. *Note*: TD denotes the theoretical density of Al_2O_3, SPS denotes spark plasma sintering and HP denotes hot pressing.

Materials (our work)			Sintering conditions	Relative density (%TD)	Electrical conductivity, σ (S/m)	
Percentage of catalyst in Al_2O_3	CNT content (wt.%)	CNT content (vol%)	SPS temperature (°C)		Measured temperature	
					77 K	280 K
0	0	0	1150	89.7	$\sim10^{-10}$ [19]	
		0	1450	98.2		
1.0	7.39	11.69	1150	55.2	211	288
		12.81	1450	79.1	586	705
2.0	8.25	13.10	1150	66.0	591	749
		14.30	1450	68.8	1642	1898
3.0	18.82	29.78	1150	57.4	1670	2009
		32.62	1450	60.2	2139	2623
4.0	19.1	30.22	1150	58.2	2012	2460
		33.12	1450	59.7	2776	3336

Materials (related works)	SPS conditions	%TD	σ (S/m)
5.7 vol% SWCNT–Al_2O_3 [23]	SPS 1150 °C/3 min	100	1050
10 vol% SWCNT–Al_2O_3 [23]	SPS 1150 °C/3 min	100	1510
15 vol% SWCNT–Al_2O_3 [17]	SPS 1150 °C/3 min	99	3345
8.5 vol% CNT/4.3 vol% Fe/Al_2O_3 [16]	HP 1500 °C/15 min	88.7	40–80
10 vol% CNT/4.3 vol% Fe/Al_2O_3 [16]	HP 1500 °C/15 min	87.5	280–400
24.48 vol% CNT–1.34 vol% Co/1.16 vol% Mo–$MgAl_2O_4$ [18]	HP 1300 °C	68.0	853

the composites sintered at high temperature of 1450 °C (images b and d) have low porosity. The intimate contact between CNTs and Al_2O_3 grains in the composites sintered at high temperature will contribute to the better electrical properties of the composites. The loose network and entangling network of CNTs in the composites are indicated in Fig. 3b.

3.2. Electrical conductivity

The electrical conductivity of the CNT–Al_2O_3 nanocomposite was measured using a four-point-probe technique. The electrical conductivity at 77 and 280 K for 7.39, 8.25, 18.82, and 19.10 wt.% CNT–Al_2O_3 nanocomposites sintered at 1150 and 1450 °C are listed in Table 1. Fig. 4 shows the temperature dependence of the electrical conductivities of these samples. The pure alumina that has an extremely low electrical conductivity in the range of 10^{-10}–10^{-12} S/m [23] is an insulator. Fig. 4 shows that the electrical conductivity of CNT–Al_2O_3 nanocomposite changes significantly even with the addition of small amount of CNTs. The electrical conductivity increases with the increase of CNT content in the nanocomposite. The dependence of electrical conductivity on the CNT content in our CNT–Al_2O_3 nanocomposite is consistent with the reported results of CNT–polymer composites in which the electrical conductivity is always enhanced and exhibits percolation behavior [2,13–15]. However, our result is in contrast to that in the reported CNT–metal–matrix composite in which the electrical conductivity decreases with the increase of the CNT content [24,25]. We suppose that this discrepancy is primarily due to the position of CNTs in the composite ceramics, i.e., whether the CNTs are in the grain boundary or in the bulk grain. In the former situation, CNTs existing in the grain boundary will connect and form a conductive network to transport electrons even at very low content [17]. However, for the later situation as in CNT–metal–matrix composites, CNTs will not be effectively interconnected and form conductive channels. Thus, percolation behavior is not presented leading to the decrease in electrical conductivity with an increase in the CNT concentration.

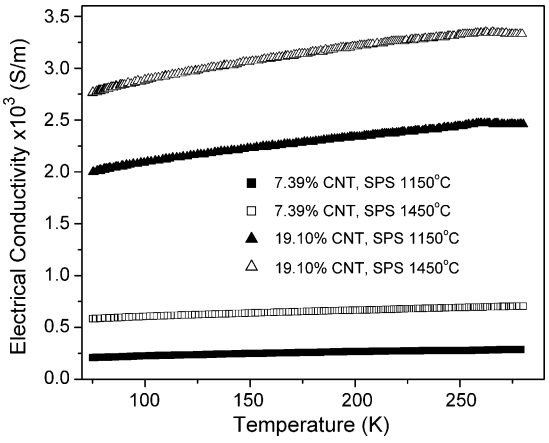

Fig. 4. Temperature dependence of electrical conductivity of CNT–Al_2O_3 nanocomposites with different CNT contents and sintered at various SPS temperatures.

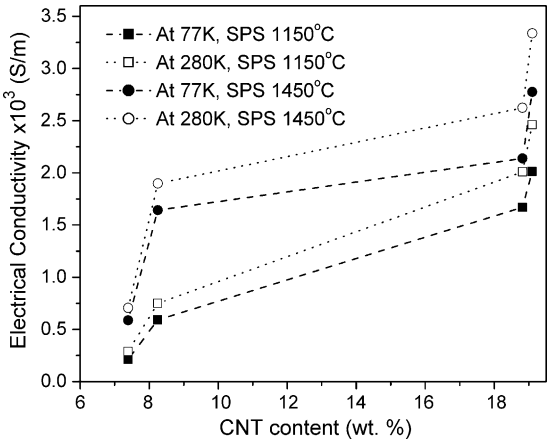

Fig. 5. Electrical conductivity as a function of CNT content in the CNT–Al_2O_3 nanocomposites at 77 and 280 K for samples sintered at 1150 and 1450 °C.

From Fig. 4, it can be seen that the 19.10 wt.% CNT–Al_2O_3 composites has the highest electrical conductivity among all the tested samples. This is reasonable because it contains the highest CNT content. The highest electrical conductivity is 2776 S/m at 77 K and 3336 S/m at 280 K for the 19.10 wt.% CNT–Al_2O_3 composite sintered at 1450 °C. Fig. 4 shows clearly that the electrical conductivity of different samples increases with the increase of the temperature, which is also different from the transport behavior of the metal–matrix composites containing CNTs [24]. The electrical conductivity of our CNT–Al_2O_3 nanocomposites falls in the range of that of the semiconductor [23]. Comparing with the pure alumina, the 19.10 wt.% CNT–Al_2O_3 shows a nearly 13 orders of magnitude increase in the electrical conductivity.

Fig. 5 shows a plot of the electrical conductivity at 77 and 280 K for CNT–Al_2O_3 nanocomposites with different CNT contents and sintered at 1150 and 1450 °C, respectively. In general, at the same SPS temperature, the conductivity increases with the increase of the CNT content in the nanocomposites. The increase of the conductivity with CNT content is explicable because the more CNTs inside the composite, the more chance for CNTs to form network in the composite, which will significantly improve the electrical conductivity of the nanocomposites. On the other hand, at the same CNT content, the conductivity of the composites increases with the sintering temperature which is evident from the results shown in Fig. 5. For instance, at measured temperature of 280 K, the sample containing 7.39 wt.% CNTs has an electrical conductivity of 288 S/m when sintered at 1150 °C, whereas the sample containing the same amount of CNTs but sintered at 1450 °C has an electrical conductivity of 705 S/m. The observed increase in the electrical conductivity can be attributed to the nanocomposite bulk density, which increases with the sintering temperature. When the as-synthesized CNT bundles are further compressed at higher sintering temperature, the spacing between nanotubes will be reduced. The spacing reduction will thus enhance the tunneling effect of electron transport between nanotubes or bundles.

Table 1 lists the comparable electrical conductivity values of the present work and the related ceramic-based CNT

nanocomposites. Flahaut et al. [16] reported the electrical conductivity of ~400 S/m for the 10 vol% CNT–Fe–alumina composite hot pressed at 1500 °C. The electrical conductivity of 850 S/m was reported for the 24.48 vol% CNT–Co/Mo–$MgAl_2O_4$ hot pressed at 1300 °C by Rul et al. [18], and 3345 S/m for the 15 vol% SWCNT–alumina nanocomposite sintered by SPS at 1150 °C by Zhan et al. [17]. The CNT volume percentage in our CNT–Al_2O_3 composite is calculated assuming the MWCNT density is the same as the graphite density of 2.25 g/cm^3 (see Table 1). At similar CNT content, the electrical conductivity of our MWCNT–alumina nanocomposite is lower than that of SWCNT–alumina composites [17] but much higher than that of the reported MWCNT–ceramic composites [16,19]. The significant enhancement in the electrical conductivity in our CNT–alumina nanocomposite can be attributed to a percolation phenomenon between CNTs or CNT bundles in alumina matrix. Due to the very high aspect ratio of the CNT (>10^4) [16], even small amount of CNTs can make the percolation possible. As the fraction of CNTs increases, the average distance between CNTs becomes small enough to make a better physical contact and hence facilitate the easy flow of electrons tunneling through the CNT bundles. Rul et al. [18] found a low percolation threshold of 0.64 vol% of double-walled CNT in CNT–$MgAl_2O_4$ composites. Ahmad et al. [19] reported a percolation threshold for 0.79 vol% of large diameter MWCNTs in CNT–Al_2O_3 nanocomposite. Moreover, the CNTs or CNT bundles in alumina matrix form a three-dimensional network and hence contribute to the enhancement of electrical conductivity of the composites. However, in the present work the electrical conductivity of nanocomposite samples with only four different CNT contents are investigated. Due to the drastic increase in CNT content in the nanocomposites synthesized with Co/Al_2O_3 content >2 wt.%, the variation in electrical conductivity with the CNT content does not follow any preferable trend to fit in the scaling law [18] to determine the percolation threshold.

Other factors related to the enhanced electrical properties in the CNT–Al_2O_3 nanocomposite include the microstructure of CNT. Indeed, the electrical conductivity of SWCNTs depends on the chirality of the graphene sheet [26], while MWCNTs are mostly electrically conductive at low temperatures [27]. During the SPS process, the sintering temperatures, durations, and pressure should be optimized to retain the high-quality CNTs. From the SEM images in Fig. 3 it is evident that even after SPS treatment (sintering temperature of 1150 and 1450 °C) the CNTs still remain intact to the large extent. The survival of CNT bundles after SPS treatment contributes significantly to the enhancement of the electrical conductivity.

The bulk density of our CNT–alumina nanocomposite is lower than that of SWCNT–alumina composite [17] and CNT–Fe–alumina composite [16], where the low density is usually attributed to the presence of open pores in the bulk material. In the present work, the density of the CNT–Al_2O_3 nanocomposites increases with the increase of the CNT content to a maximum, and then decreases for further increase in the CNT content. The reduction of density in the CNT–ceramic composite has been reported [16,17], but its exact interaction mechanism has not been fully understood. In terms of the densification process of ceramics, elimination of pore and mass transportation through bulk diffusion or surface diffusion are two basic but crucial factors to determine the ultimate density. Therefore, the effect of CNTs on the sintering property of composite ceramics should be mainly interpreted from these two points. Although little work has been carried out to elucidate their relationship, it is assumed that CNTs existing in grain boundaries act as space barriers to prevent closing up of grains. Mass transportation is accordingly inhibited. Thus, nano size or sub-micron size grains were maintained in the final ceramics. Previous work on SWCNT–Al_2O_3 nanocomposites [17] with largely enhanced fracture toughness is a good example of this case, in which the unique entangling network was constructed by loading SWCNTs into the intergranular spaces of Al_2O_3 ceramics.

As previously reported [16], CNTs greatly inhibit the matrix grain growth, which is very unfavorable to the densification when the CNT content is too high. Also, CNTs probably inhibit the uniaxial pressure action owing to their elastic behavior. These phenomena are particularly effective in the present samples in which, due to the in situ synthesis of CNT, all the matrix grain are surrounded by the webs of CNTs. These results confirm that the influence of CNT on the matrix microstructure and densification is more and more pronounced when the CNT content is increased [18]. Our composite samples sintered at higher SPS temperatures (1450 °C) and even with low relative density (<80%) show appreciable enhancement of electrical conductivity with an increase in the CNT content. This can occur because CNTs and CNT bundles which are located in those open pores are probably interconnected without significant interaction with the oxide matrix and thus are less damaged than CNTs located at the matrix grain boundary or captured by the matrix grain [18], and the retained CNTs will thus significantly enhance the electrical conductivity in the CNT–ceramic composite. Hence, synthesis route, SPS conditions, and CNT and ceramic characteristics optimized together can probably concur to a lesser damaging to CNTs. In the future, we aim at investigating the enhancement mechanism of the electrical properties of CNT–alumina nanocomposites induced by the CNTs and to further improve the electrical properties of the nanocomposites.

4. Conclusion

CNT–alumina nanocomposites have been successfully synthesized using CVD technique and densified by SPS. The MWCNTs with diameters in the range of 10–40 nm have been grown directly in the alumina powder and thus the as-grown CNTs are homogeneously distributed within the alumina matrix. The electrical properties are highly dependent on the CNT content, bulk density, and SPS conditions. The electrical conductivity of CNT–alumina nanocomposites are in the range of that of semiconductor, with a maximum conductivity of 3336 S/m at near room temperature in the 19.10 wt.% CNT–Al_2O_3 sintered at 1450 °C. Electrical conductivity increases with the increase of the CNT content and the sintering

temperature. The significant enhancement of electrical conductivity can be attributed to the percolation phenomena between CNTs or CNT bundles in the alumina matrix and the density of the composite. The composition, element distribution, and microstructure are predominant factors determining the electrical properties of the CNT–ceramic composites.

Acknowledgements

W.Z. Li and Q.W. Wang acknowledge the support from the Air Force Office of Scientific Research Small Business Technology Transfer (STTR) Funding (contract numbers: FA9550-05-C-0126 for Phase I and FA9550-06-C-0136 for Phase II). W.Z. Li would also like to acknowledge the support from the National Science Foundation under grant DMR-0548061.

References

[1] P.M. Ajayan, L.S. Schadler, C. Giannaris, A. Rubio, Single-walled carbon nanotube–polymer composites: strength and weakness, Adv. Mater. 12 (2000) 750–753.
[2] B.E. Kilbride, J.N. Coleman, J. Fraysse, P. Fournet, M. Cadek, A. Drury, S. Hutzler, S. Roth, W.J. Blau, Experimental observation of scaling laws for alternating current and direct current conductivity in polymer–carbon nanotube composite thin films, J. Appl. Phys. 92 (2002) 4024–4030.
[3] M.J. Biercuk, M.C. Llaguno, M. Radosavlijevic, J.K. Hyun, A.T. Johnson, Carbon nanotube composites for thermal management, Appl. Phys. Lett. 80 (2002) 2767–2769.
[4] A. Peigney, Ch. Laurent, E. Flahaut, A. Rousset, Carbon nanotubes in novel ceramic matrix nanocomposites, Ceram. Int. 26 (2000) 677–683.
[5] G. Van Lier, C. Van Alsenoy, V. Van Doren, P. Geerlings, Ab initio study of the elastic properties of single-walled carbon nanotubes and graphene, Chem. Phys. Lett. 326 (2000) 181–185.
[6] M.M.J. Treacy, T.W. Ebbesen, J.M. Gibson, Exceptionally high Young's modulus observed for individual carbon nanotubes, Nature 381 (1996) 678–680.
[7] M.F. Yu, O. Lourie, M.J. Dyer, K. Moloni, T.F. Kelly, R.S. Ruoff, Strength and breaking mechanism of multiwalled carbon nanotubes under tensile load, Science 287 (2000) 637–640.
[8] A. Thess, R. Lee, P. Nikolaev, H. Dai, P. Petit, J. Robert, C. Xu, Y.H. Lee, S.G. Kim, A.G. Rinzler, D.T. Colbert, G.E. Scuseria, D. Tomanek, J.E. Fischer, R.E. Smalley, Crystalline ropes of metallic carbon nanotubes, Science 273 (1996) 483–487.
[9] Y. Ando, X. Zhaoa, H. Shimoyama, G. Sakai, K. Kaneto, Physical properties of multiwalled carbon nanotubes, Int. J. Inorg. Mater. 1 (1999) 77–82.
[10] R.H. Baughman, A.A. Zakhidov, W.A. de Heer, Carbon nanotubes—the route toward applications, Science 297 (2000) 787–792.
[11] K.M. Prewo, Fiber-reinforced ceramics: new opportunities for composite materials, Am. Ceram. Soc. Bull. 68 (1989) 395–400.
[12] G.D. Zhan, J.D. Kuntz, J. Wan, A.K. Mukherjee, Single-wall carbon nanotubes as attractive toughening agents in alumina-based nanocomposites, Nat. Mater. 2 (2003) 38–42.
[13] E. Kymakis, G.A.J. Amaratunga, Electrical properties of single-wall carbon nanotube–polymer composite films, J. Appl. Phys. 99 (2006) 084302.
[14] S. Barrau, P. Demont, A. Peigney, Ch. Laurent, C. Lacabanne, DC and AC conductivity of carbon nanotubes–polyepoxy composites, Macromolecules 36 (2003) 5187–5194.
[15] J.K.W. Sandler, J.E. Kirk, I.A. Kinloch, M.S.P. Shaffer, A.H. Windle, Ultra-low electrical percolation threshold in carbon-nanotube–epoxy composites, Polymer 44 (2003) 5893–5899.
[16] E. Flahaut, A. Peigney, Ch. Laurent, C. Marlière, F. Chastel, A. Rousset, Carbon nanotube–metal-oxide nanocomposites: microstructure, electrical conductivity and mechanical properties, Acta Mater. 48 (2000) 3803–3812.
[17] G.D. Zhan, J.D. Kuntz, E. Garay, A.K. Mukherjee, Electrical properties of nanoceramics reinforced with ropes of single-walled carbon nanotubes, Appl. Phys. Lett. 83 (2003) 1228–1230.
[18] S. Rul, F. Lefèvre-schlick, E. Capria, Ch. Laurent, A. Peigney, Percolation of single-walled carbon nanotubes in ceramic matrix nanocomposites, Acta Mater. 52 (2004) 1061–1067.
[19] K. Ahmad, W. Pan, S.-L. Shi, Electrical conductivity and dielectric properties of multiwalled carbon nanotube and alumina composites, Appl. Phys. Lett. 89 (2006) 133122.
[20] W.Z. Li, J.G. Wen, M. Sennett, Z.F. Ren, Clean double-walled carbon nanotubes synthesized by CVD, Chem. Phys. Lett. 368 (2003) 299–306.
[21] R. Khare, S. Bose, Carbon nanotube-based composites—a review, J. Miner. Mater. Charact. Eng. 4 (2005) 31–46.
[22] S.B. Sinnott, R. Andrews, D. Qian, A.M. Rao, Z. Mao, E.C. Dickey, F. Derbyshire, Model of carbon nanotube growth through chemical vapor deposition, Chem. Phys. Lett. 315 (1999) 25–30.
[23] G.D. Zhan, A.K. Mukherjee, Carbon nanotube reinforced alumina-based ceramics with novel mechanical, electrical, and thermal properties, Int. J. Appl. Ceram. Technol. 1 (2004) 161–171.
[24] C.L. Xu, B.Q. Wei, R.Z. Ma, J. Liang, X.K. Ma, D.H. Wu, Fabrication of aluminum–carbon nanotube composites and their electrical properties, Carbon 37 (1999) 855–858.
[25] Q. Huang, L. Gao, Manufacture and electrical properties of multiwalled carbon nanotube/$BaTiO_3$ nanocomposite ceramics, J. Mater. Chem. 14 (2004) 2536–2541.
[26] A.B. Kaiser, G. Düsberg, S. Roth, Heterogeneous model for conduction in carbon nanotubes, Phys. Rev. B 57 (1998) 1418–1421.
[27] J.W.G. Wildöer, L.C. Venema, A.G. Rinzler, R.E. Smalley, C. Dekker, Electronic structure of atomically resolved carbon nanotubes, Nature 391 (1998) 59–62.